Available online at www.sciencedirect.com
ScienceDirect
Chinese Journal of Aeronautics 23(2010) 364-369
Chinese Journal of Aeronautics
www.elsevier.com/locate/cja

A Distributed Coordinated Control Scheme for Morphing Wings with Sampled Communication

Wu Jun, Lu Yuping*

College of Automation Engineering, Nanjing University of Aeronautics and Astronautics, Nanjing 210016, China

Received 10 June 2009; accepted 27 October 2009

Abstract

To investigate the control of morphing wings by means of interacting effectors, this article proposes a distributed coordinated control scheme with sampled communication on the basis of a simple morphing wing model, established with arrayed agents. The control scheme can change the shape of airfoil into an expected one and keep it smooth during morphing. As the interconnection of communication network and the agents would make the behavior of the morphing wing system complicated, a diagrammatic stability analysis method is put forward to ensure the system stability. Two simulations are carried out on the morphing wing system by using MATLAB. The results stand witness to the feasibility of the distributed coordinated control scheme and the effectiveness of the diagrammatic stability analysis method.

Keywords: morphing wing; multi agent systems; distributed control; coordinated control; system stability

1. Introduction

Morphing aircraft are able to accomplish many kinds of missions, perform radically new maneuver not realized with conventional control surfaces, economize more fuel consumption and provide reduced radar cross section.

Many morphing research programs have been conducted abroad, such as the mission adaptive wing (MAW) research program[1], the active flexible wing (AFW) program[2], the active aeroelastic wing (AAW) research program[3], the morphing aircraft structures (MAS) program[4], and the active aeroelastic aircraft structures (3AS)[5]. Most of them adopted arrays of interacting effectors instead of conventional ailerons, flaps or rudders. These effectors can produce shape changes or bumps on the surface of an airfoil to generate control moments.

Nevertheless, the adoption of arrayed interacting effectors also causes new problems. First, in order to accomplish cooperative tasks, the effectors must exchange information among themselves through the communication network. Thus, the morphing wing system should behave with both continuous and discrete dynamic characteristics. Effectors have continuous dynamics and due to the limited data rate in the channel, controllers make discrete decisions on what information to transmit and when to send it. Second, the behavior of morphing wing system depends not only on the individual effector's dynamics, but also on the nature of their interconnection. This increases the difficulty in analyzing system stability. Third, the real-time control of the morphing wing system requires a strong communication and computation capability to support it. Obviously, with this being the situation, a conventional centralized control can hardly be satisfactorily employed. What's more, the non-negligible communication time delays might make the system unstable.

In existing morphing wing systems, coordinated control techniques for arrayed effectors have attracted little attention. D. Liberzon[6] applied Lyapunov stability theorem for hybrid systems. It requires that the derivative of Lyapunov function is negative definite when the system is stable. However, the derivative of Lyapunov function is negative semidefinite in our study. J. A. Fax, et al.[7] investigated cooperative control and information flow of vehicle formations. Based on his research, T. H. Kim, et al.[8] developed a distributed formation control scheme for multi-agent continuous-time dynamical systems with sampled communication. But it is only suitable to control single input single output (SISO) systems.

*Corresponding author. Tel.: +86-25-84891842
E-mail address: yplac@nuaa.edu.cn
Foundation item: National Natural Science Foundation of China (90605007)

doi: 10.1016/S1000-9361(09)60228-4

After having investigated the problems mentioned above, the article develops a distributed coordinated control scheme, which keeps the airfoil deforming smoothly in the process of its reaching an expected shape. This approach proves more realistic and practical than any other method in the existing literature. And a simple diagrammatic stability analysis method is also presented herein.

2. Morphing Wing Model

The innovative control effector (ICE) aircraft[9] uses arrays of shape changing effectors, which are grouped into equivalent surfaces for generating control forces. Fig.1 shows the four distributed shape-change device arrays for the ICE configuration. The entire set of shape-change device arrays includes 156 individual devices in total, halved by two wings.

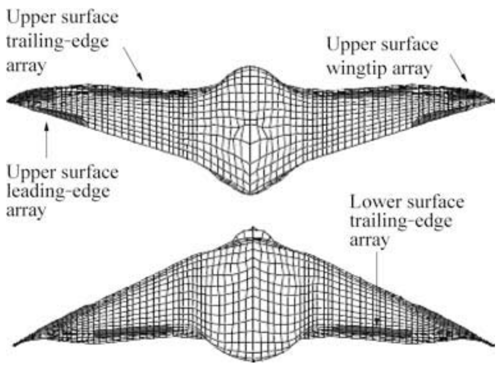

Fig.1 Effector arrays for ICE configuration.

In order to investigate the control scheme, a variable camber and thickness wing model is established with device arrays (see Fig.2). It is a multi agent system. Every agent comprises an electromechanical actuator together with sensors and a local controller. A light plate, where arrayed agents are located, is secured in the middle of the wing. Covered by a skin, the electromechanical actuators deform the airfoil by their movements. Agents transmit sensed local information to adjacent agents through controller area network (CAN) bus. Abiding by the control law and the received information, the local controller generates control forces and moments to drive the electromechanical actuators. This way, the morphing wing system constitutes a closed-loop control structure.

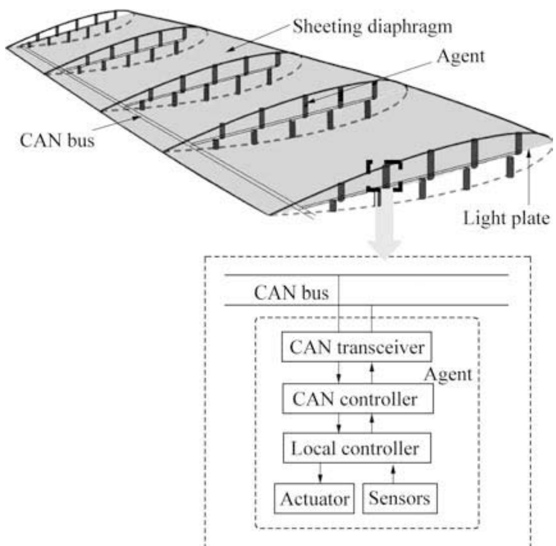

Fig.2 Structure diagram of a morphing wing.

This article assumes there being an array of $m\times n$ agents on the upper surface of the light plate (see Fig.3). All the agents are numbered from 1 to mn, i.e., $P_1, P_2, \cdots, P_{mn}$.

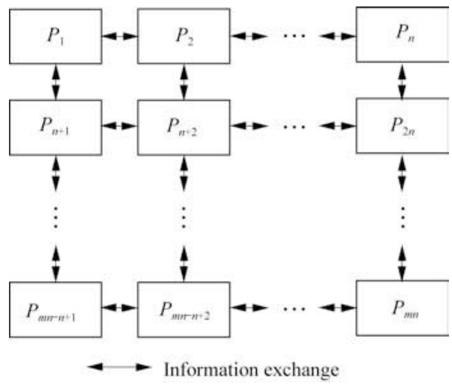

Fig.3 A schematic diagram showing contiguity of agents.

Let $a = 1/T_{\mathrm{m}} > 0$, $b = K_{\mathrm{PWM}}K_{\mathrm{m}}/(i_{\mathrm{m}}T_{\mathrm{m}}) > 0$, where T_{m} is the electromechanical time constant of the actuator, K_{m} the transfer coefficient of the actuator, K_{PWM} the equivalent gain of the pulse width modulation (PWM) driver and i_{m} the reduction ratio.

Suppose that the continuous-time system dynamics of the ith agent is

$$\left.\begin{aligned} \dot{\boldsymbol{x}}_i(t) &= \begin{bmatrix} 0 & 1 \\ 0 & -a \end{bmatrix} \boldsymbol{x}_i(t) + \begin{bmatrix} 0 \\ b \end{bmatrix} u_i(t) \\ \boldsymbol{y}_i(t) &= \boldsymbol{x}_i(t) \end{aligned}\right\} \quad (1)$$

where $\boldsymbol{x}_i = [\overline{r}_i \quad v_i]^{\mathrm{T}} \in \mathbf{R}^2$ is the state of P_i, $\overline{r}_i = r_i - r_i^{\mathrm{d}}$ ($r_i \in \mathbf{R}$) the displacement, $r_i^{\mathrm{d}} \in \mathbf{R}$ the target displacement, and $v_i \in \mathbf{R}$ the velocity of P_i, $u_i \in \mathbf{R}$ the control input of P_i and $\boldsymbol{y}_i \in \mathbf{R}^2$ its system output.

The state space equation Eq.(1) can also be written in the form of the transfer function as follows:

$$\left.\begin{aligned} \boldsymbol{y}_i(s) &= \left[\overline{r}_i(s) \quad v_i(s)\right]^{\mathrm{T}} = \boldsymbol{H}(s)u_i(s) \\ \boldsymbol{H}(s) &= \begin{bmatrix} \dfrac{b}{s(s+a)} & \dfrac{b}{s+a} \end{bmatrix}^{\mathrm{T}} \end{aligned}\right\} \quad (2)$$

3. Distributed Coordinated Control Scheme

Because the information the agents receive is far more than what the limited channel capacity could do in such a system, the conventional centralized control is no longer fit for the use. This leads to the necessity of considering a distributed control scheme as depicted in Fig.4.

The output of an agent is sampled every T s, where T ($T>0$) is a fixed sampling period. The sampled data are transmitted to adjacent agents with communication time delay, τ (unit: s), an integral multiple of T. When the local controller receives the sampled data from all the adjacent agents, it generates the control force. The zero-order holder generates continuous input signals by retaining the discrete control force signals constant over the period T.

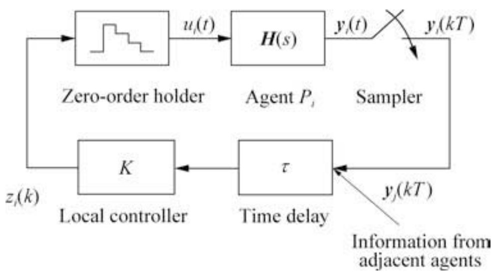

Fig.4 Block diagram of distributed control system.

The distributed coordinated control law is given by

$$z_i(k)=-\frac{1}{b}[k_{\rm g}\quad d_{\rm g}]\boldsymbol{y}_i(kT)-\frac{1}{b}[k_{\rm s}\quad d_{\rm s}]\sum_{j\in\Im_i}[\boldsymbol{y}_i(kT)-\boldsymbol{y}_j(kT)] \tag{3}$$

where $k_{\rm g}>0$, $d_{\rm g}>0$, $k_{\rm s}\geq 0$, $d_{\rm s}\geq 0$ and the set $\Im_i\subset[1,mn]\backslash\{i\}$ represents the set of agents adjacent to the ith agent.

The first term of Eq.(3) is used to drive the agent to the target displacement. If a certain agent moves rather faster than the adjacent agents, the skin might break up. So, it is necessary to use the second term of Eq.(3) to match the displacement change and velocity change of adjacent agents so as to keep the airfoil deforming smoothly.

The control input is

$$u_i(t)=z_i(k),\ t\in[kT+\tau,(k+1)T+\tau] \tag{4}$$

4. System Stability Analysis

Let

$$\boldsymbol{x}(t)=\begin{bmatrix}\boldsymbol{x}_1^{\rm T}(t) & \boldsymbol{x}_2^{\rm T}(t) & \cdots & \boldsymbol{x}_{mn}^{\rm T}(t)\end{bmatrix}^{\rm T}$$
$$\boldsymbol{y}(t)=\begin{bmatrix}\boldsymbol{y}_1^{\rm T}(t) & \boldsymbol{y}_2^{\rm T}(t) & \cdots & \boldsymbol{y}_{mn}^{\rm T}(t)\end{bmatrix}^{\rm T}$$
$$\boldsymbol{u}(t)=\begin{bmatrix}u_1(t) & u_2(t) & \cdots & u_{mn}(t)\end{bmatrix}^{\rm T}$$
$$\boldsymbol{z}(k)=\begin{bmatrix}z_1(k) & z_2(k) & \cdots & z_{mn}(k)\end{bmatrix}^{\rm T}$$

Then, the dynamics of the morphing wing system can be represented by

$$\left.\begin{aligned}\dot{\boldsymbol{x}}(t)&=\left(\boldsymbol{I}_{mn}\otimes\begin{bmatrix}0&1\\0&-a\end{bmatrix}\right)\boldsymbol{x}(t)+\left(\boldsymbol{I}_{mn}\otimes\begin{bmatrix}0\\b\end{bmatrix}\right)\boldsymbol{u}(t)\\ \boldsymbol{y}(t)&=\boldsymbol{x}(t)\end{aligned}\right\} \tag{5}$$

where $\otimes$ represents Kronecker product, and $\boldsymbol{I}_N\in\mathbf{R}^{N\times N}$ identity matrix.

The distributed coordinated control scheme for the morphing wing system can be represented by

$$\boldsymbol{z}(k)=-\frac{1}{b}(\boldsymbol{I}_{mn}\otimes[k_{\rm g}\quad d_{\rm g}])\boldsymbol{y}(kT)-\frac{1}{b}(\boldsymbol{I}_{mn}\otimes[k_{\rm s}\quad d_{\rm s}])(\boldsymbol{L}\otimes\boldsymbol{I}_2)\boldsymbol{y}(kT) \tag{6}$$

$$\boldsymbol{u}(t)=\boldsymbol{z}(k),\ t\in[kT+\tau,(k+1)T+\tau) \tag{7}$$

where $\boldsymbol{L}\in\mathbf{R}^{mn\times mn}$ is a conjugate matrix, in which $L(i,j)=-1(j\in\Im_i)$, $L(i,i)$ the number of agents adjacent to the ith agent and the other elements of $\boldsymbol{L}$ equal 0.

Theorem 1 Consider an array of mn agents given by Eq.(1) and a distributed coordinated control scheme defined as Eqs.(3)-(4). Let

$$g_i(z)=(k_{\rm g}+\lambda_i k_{\rm s})\frac{Tz^{-\tau/T}}{a(z-1)}+\left(d_{\rm g}+\lambda_i d_{\rm s}-\frac{k_{\rm g}+\lambda_i k_{\rm s}}{a}\right)\frac{(1-{\rm e}^{-aT})z^{-\tau/T}}{a(z-{\rm e}^{-aT})}$$

where λ_i is the eigenvalue of $\boldsymbol{L}$. Map the polar coordinates of $g_i(z)$ as z varies from ${\rm e}^{0j}$ to ${\rm e}^{2\pi j}$ while skip all possible poles of $g_i(z)$ on the unit circle of the z plane. Then the morphing wing system Eq.(5) is stable if and only if all the intersection points of $g_i(z)$ with the real axis are to the right of the point $(-1,0)$ for $i=1, 2, \cdots, mn$.

Proof From Eq.(3), it is observed that there is an interaction between the agents. Hence, a Schur transformation has to be used to decouple it.

Let $\boldsymbol{Q}$ be the Schur transformation of $\boldsymbol{L}$, then the unitary matrix is

$$\boldsymbol{Q}^{\rm H}\boldsymbol{L}\boldsymbol{Q}={\rm diag}(\lambda_1,\lambda_2,\cdots,\lambda_{mn})$$

Let

$$\tilde{\boldsymbol{x}}(t)=(\boldsymbol{Q}\otimes\boldsymbol{I}_2)^{-1}\boldsymbol{x}(t),\quad \tilde{\boldsymbol{y}}(t)=(\boldsymbol{Q}\otimes\boldsymbol{I}_2)^{-1}\boldsymbol{y}(t)$$
$$\tilde{\boldsymbol{u}}(t)=(\boldsymbol{Q}\otimes\boldsymbol{I}_1)^{-1}\boldsymbol{u}(t),\quad \tilde{\boldsymbol{z}}(k)=(\boldsymbol{Q}\otimes\boldsymbol{I}_1)^{-1}\boldsymbol{z}(k)$$

then Eqs.(5)-(7) can be rewritten into

$$\left.\begin{aligned}\dot{\tilde{\boldsymbol{x}}}(t)&=\left(\boldsymbol{I}_{mn}\otimes\begin{bmatrix}0&1\\0&-a\end{bmatrix}\right)\tilde{\boldsymbol{x}}(t)+\left(\boldsymbol{I}_{mn}\otimes\begin{bmatrix}0\\b\end{bmatrix}\right)\tilde{\boldsymbol{u}}(t)\\ \tilde{\boldsymbol{y}}(t)&=\tilde{\boldsymbol{x}}(t)\end{aligned}\right\} \tag{8}$$

$$\tilde{\boldsymbol{z}}(k)=-\frac{1}{b}(\boldsymbol{I}_{mn}\otimes[k_{\rm g}\quad d_{\rm g}])\tilde{\boldsymbol{y}}(kT)-\frac{1}{b}({\rm diag}(\lambda_1,\lambda_2,\cdots,\lambda_{mn})\otimes[k_{\rm s}\quad d_{\rm s}])\tilde{\boldsymbol{y}}(kT) \tag{9}$$

$$\tilde{\boldsymbol{u}}(t)=\tilde{\boldsymbol{z}}(k),\ t\in[kT+\tau,(k+1)T+\tau) \tag{10}$$

Because Eqs.(8)-(10) are all of block diagonal type, system stability is equivalent to the stability of the defined mn subsystems using the diagonal blocks. Thus, the agent and the control scheme can be rewritten into

$$\left.\begin{aligned}\dot{\tilde{\boldsymbol{x}}}_i(t)&=\begin{bmatrix}0&1\\0&-a\end{bmatrix}\tilde{\boldsymbol{x}}_i(t)+\begin{bmatrix}0\\b\end{bmatrix}\tilde{u}_i(t)\\ \tilde{\boldsymbol{y}}_i(t)&=\tilde{\boldsymbol{x}}_i(t)\end{aligned}\right\}\qquad(11)$$

$$\tilde{z}_i(k)=-\frac{1}{b}[k_\mathrm{g}+\lambda_i k_\mathrm{s}\quad d_\mathrm{g}+\lambda_i d_\mathrm{s}]\tilde{\boldsymbol{y}}_i(kT)\qquad(12)$$

$$\tilde{u}_i(t)=\tilde{z}_i(k),\ t\in[kT+\tau,(k+1)T+\tau)\qquad(13)$$

Hence, the morphing wing system in Eqs.(5)-(7) is stable if and only if every system in Eqs.(11)-(13) is stable simultaneously.

Let discrete-time transfer function derived from $\boldsymbol{H}(s)$ be $\boldsymbol{H}(z)$, then $\boldsymbol{H}(s)$ is equivalent to $\boldsymbol{H}(z)$ via zero-order holder, which is expressed as

$$\boldsymbol{H}(z)=(1-z^{-1})Z\left\{\frac{\boldsymbol{H}(s)}{s}\right\}$$

where Z denotes the z-transform.

The closed-loop transfer function of the ith agent is

$$\left(\boldsymbol{I}_2+\frac{z^{-\tau/T}}{b}\boldsymbol{H}(z)[k_\mathrm{g}+\lambda_i k_\mathrm{s}\quad d_\mathrm{g}+\lambda_i d_\mathrm{s}]\right)^{-1}\boldsymbol{H}(z)\qquad(14)$$

If $\overline{r_i}$ is stable, obviously, $v_i=\dot{\overline{r_i}}$ is stable as well. Therefore, only the stability of $\overline{r_i}$ needs to be considered. From Eq.(14), the following can be obtained

$$\frac{\overline{r_i}(z)}{u_i(z)}=\frac{\dfrac{b}{a}\left[\dfrac{T}{z-1}-\dfrac{1-\mathrm{e}^{-aT}}{a(z-\mathrm{e}^{-aT})}\right]}{1+g_i(z)}$$

where

$$\left.\begin{aligned}g_i(z)&=(k_\mathrm{g}+\lambda_i k_\mathrm{s})\frac{Tz^{-\tau/T}}{a(z-1)}+\\&\left(d_\mathrm{g}+\lambda_i d_\mathrm{s}-\frac{k_\mathrm{g}+\lambda_i k_\mathrm{s}}{a}\right)\frac{(1-\mathrm{e}^{-aT})z^{-\tau/T}}{a(z-\mathrm{e}^{-aT})}=\\&\frac{(p+q)z-(\mathrm{e}^{-aT}p+q)}{a^2z^{\tau/T}(z-1)(z-\mathrm{e}^{-aT})}\\p&=aT(k_\mathrm{g}+\lambda_i k_\mathrm{s})\\q&=\left[a(d_\mathrm{g}+\lambda_i d_\mathrm{s})-(k_\mathrm{g}+\lambda_i k_\mathrm{s})\right](1-\mathrm{e}^{-aT})\end{aligned}\right\}\qquad(15)$$

$g_i(z)$ represents the open-loop transfer function of a feedback loop and $g_i(\infty)=0$.

Based on the reformulation of the Nyquist criterion for discrete systems[10], the closed-loop system is stable if and only if the following equation holds

$$W=(\alpha+2\beta)\pi\qquad(16)$$

where W denotes the angle swept by the vector $\boldsymbol{V}$ pointing from (–1,0) to the moving point $g_i(z)$ in the $g(z)$ plane, as z varies from e^{0j} to $\mathrm{e}^{2\pi j}$ while skipping all possible poles of $g_i(z)$ on the unit circle of the z plane, and the counterclockwise direction is reckoned to be positive; α denotes the number of poles of $g_i(z)$ on the unit circle of the z plane and β the number of poles of $g_i(z)$ outside the unit circle of the z plane.

From Eq.(15), it can be seen that $\alpha=1$, $\beta=0$ and $(\alpha+2\beta)\pi=\pi$. The pole of $g_i(z)$ on the unit circle of the z plane is $z=1=\mathrm{e}^{0j}$.

Polar coordinates of $g_i(z)$ are shown in Fig.5, of which Fig.5(a) and Fig.5(b) are the examples for $p+q>0$ and Fig.5(c) and Fig.5(d) for $p+q\le 0$. The number of intersection points of $g_i(z)$ and the real axis increases with τ increasing. From the polar plots, it can be seen that $W=\pi$ when all the intersection points of $g_i(z)$ and the real axis are to the right of the point (–1,0), as shown in Fig.5(a) and Fig.5(c). Otherwise, $W\ne\pi$, for instance, $W=-3\pi$ as the case in Fig.5(b) and Fig.5(d).

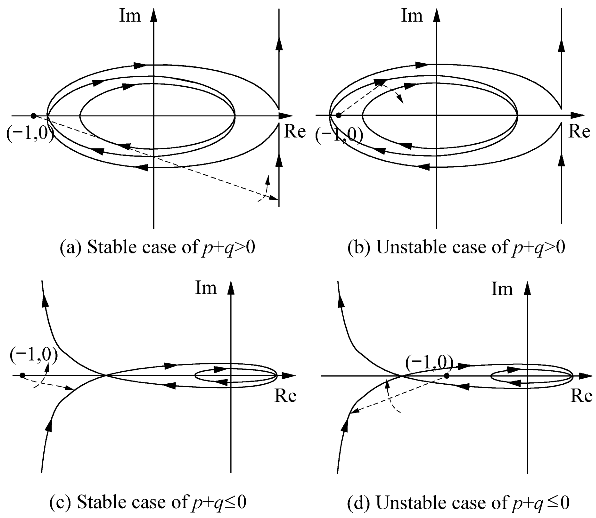

(a) Stable case of $p+q>0$ (b) Unstable case of $p+q>0$
(c) Stable case of $p+q\le 0$ (d) Unstable case of $p+q\le 0$

Fig.5 Polar plots of $g_i(z)$.

Therefore, the morphing wing system is stable if and only if the intersection points of $g_i(z)$ and the real axis are to the right of point (–1,0) for $i=1,2,\cdots,mn$.

5. MATLAB Simulations

In general, the requirement for low-altitude transonic attacks would do harm to the aircraft's ability of long-range subsonic cruising. The superiority of morphing aircraft just lies in its capability of continuously accommodating to performance demands posed by different missions during the flight. Here TrueTime toolbox of MATLAB is used to simulate the case that an aircraft changes from cruising with the airfoil of NACA 0012 to attacking with RAE 2822.

An array of 3×6 agents secured on the lower surface of a light plate is connected through CAN bus at the baud rate of 1 Mbps. The initial displacements of the agents are

$$\boldsymbol{r}_0=\begin{bmatrix}5.093&6&5.320&4.480&3.32&1.867\\4.991\,1&5.88&5.213\,6&4.390\,4&3.253\,6&1.829\,7\\4.838\,4&5.7&5.054&4.256&3.154&1.773\,6\end{bmatrix}$$

The target displacements are

$$\boldsymbol{r}^{\mathrm{d}} = \begin{bmatrix} 5.169\,4 & 5.923\,6 & 3.804\,3 & 2.449\,5 & 1.024\,4 & 0.06 \\ 5.066 & 5.805\,1 & 3.728\,2 & 2.400\,5 & 1.003\,9 & 0.058\,8 \\ 4.910\,9 & 5.627\,4 & 3.614\,1 & 2.327 & 0.973\,2 & 0.057 \end{bmatrix}$$

The agent is chosen with $i_{\mathrm{m}} = 215$ rad/m, $K_{\mathrm{m}} = 25$ rad·s/V, $K_{\mathrm{PWM}} = 576$, $T_{\mathrm{m}} = 7.5$ ms, and a sampling period $T = 0.01$ s. Hence, the state space model of the agent is

$$\dot{\boldsymbol{x}}_i = \begin{bmatrix} 0 & 1 \\ 0 & -133.3 \end{bmatrix} \dot{\boldsymbol{x}}_i + \begin{bmatrix} 0 \\ 8\,933.3 \end{bmatrix} u_i$$

Two simulations are carried out to show the distributed coordinated control scheme and the diagrammatic stability analysis method. The parameters of control schemes Eqs.(3)-(4) in the first simulation are $k_{\mathrm{s}} = k_{\mathrm{g}} = 25$, $d_{\mathrm{s}} = d_{\mathrm{g}} = 1$, $\tau = 0.01$; while those in the second simulation are $k_{\mathrm{s}} = k_{\mathrm{g}} = 8$, $d_{\mathrm{s}} = d_{\mathrm{g}} = 25$, $\tau = 0.02$. Figs.6-7 evince the polar coordinates and position trajectories of 18 agents.

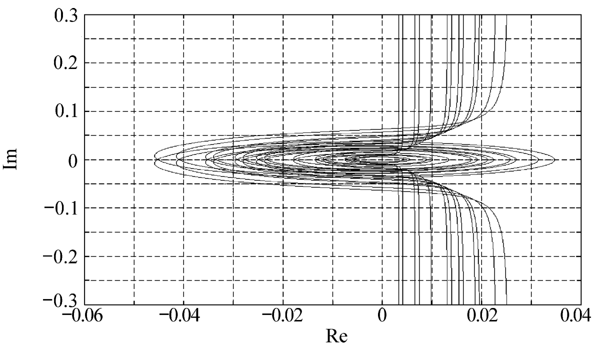

(a) Polar coordinates

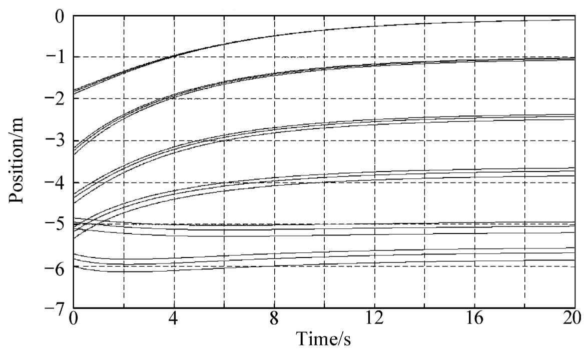

(b) Position trajectories

Fig.6 Polar coordinates and position trajectories when $k_{\mathrm{s}} = k_{\mathrm{g}} = 25$, $d_{\mathrm{s}} = d_{\mathrm{g}} = 1$, $\tau = 0.01$.

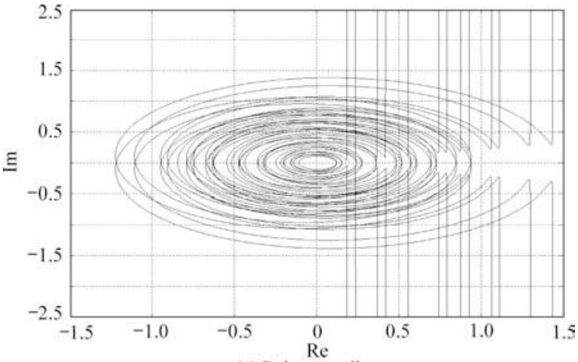

(a) Polar coordinates

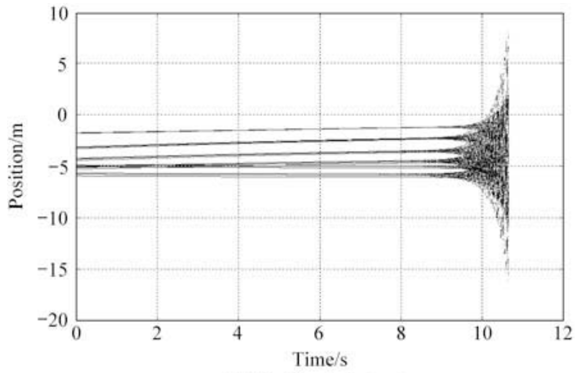

(b) Position trajectories

Fig.7 Polar coordinates and position trajectories when $k_{\mathrm{s}} = k_{\mathrm{g}} = 8$, $d_{\mathrm{s}} = d_{\mathrm{g}} = 25$, $\tau = 0.02$.

The polar plots in Fig.6 indicate that the morphing wing system is stable according to Theorem 1, and the position trajectories show that the airfoil converges to the expected shape and maintains the deformation smooth during the motion. By contrast, Fig.7 indicates the closed-loop system is unstable.

The same is true of the configurations of the lower surface. In the lower surface case, the parameters of control scheme Eqs.(3)-(4) are $k_{\mathrm{s}} = k_{\mathrm{g}} = 25$, $d_{\mathrm{s}} = d_{\mathrm{g}} = 1$, $\tau = 0.01$. Fig.8 shows the airfoil changes of a morphing wing with the interval of 10 s. Clearly, the more the agents are used, the smoother the wing surface would be kept. Fig.9 illustrates the experimental device of morphing wings developed in-house. Through MAT-

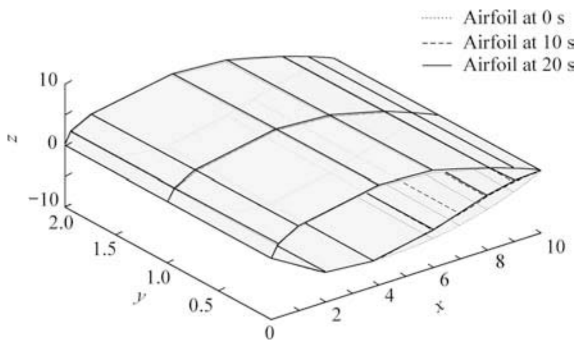

Fig.8 Shape changes of a wing every 10 s.

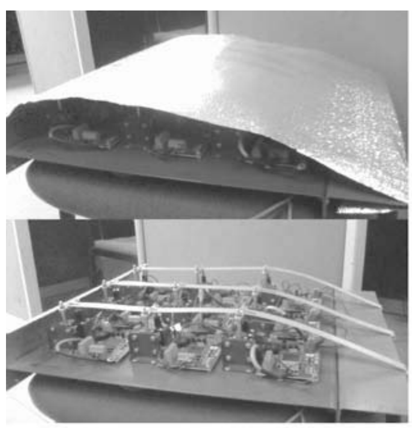

Fig.9 Experimental morphing wings with and without skins.

LAB simulations and test on the experimental device, the control scheme is rather effective in commanding the airfoil changes to achieve the desired shape.

6. Conclusions

This article presents a distributed coordinated control scheme for morphing wings. The influences of the communication network are considered in analyzing the stability of the system. And a simple diagrammatic stability analysis method has been developed. Two simulations using MATLAB have been carried out to verify the validity of the distributed coordinated control scheme and the effectiveness of the diagrammatic stability analysis method.

References

[1] Hardy R. AFTI/F-111 mission adaptive wing technology demonstration program. AIAA-1983-1057, 1983.
[2] Perry B III, Cole S R, Miller G D. A summary of the active flexible wing program. NASA-TM-107655, 1992.
[3] Pendleton E, Griffin K E, Kehoe M W. A flight research program for active aeroelastic wing technology. AIAA-1996-1574, 1996.
[4] Bowman J, Sanders B, Cannon B. Development of next generation morphing aircraft structures. AIAA-2007-1730, 2007.
[5] Schweiger J, Suleman A, Kuzmina S, et al. MDO concepts for an European research project on active aeroelastic aircraft. AIAA-2002-5403, 2002.
[6] Liberzon D. A hybrid control framework for systems with quantization. Proceedings of the 40th IEEE Conference on Decision and Control. 2001; 1217-1222.
[7] Fax J A, Murray R M. Information flow and cooperative control of vehicle formations. IEEE Transactions on Automatic Control 2004; 49(9): 1465-1476.
[8] Kim T H, Hara S. Cyclic pursuit strategy for multiagent dynamical systems with sampled communication. SICE Annual Conference. 2008; 2436-2441.
[9] Raney D L, Montgomery R C, Green L L. Flight control using distributed shape-change effector arrays. AIAA-2000-1560, 2000.
[10] Yeung K S, Lai H M. A reformulation of the Nyquist criterion for discrete systems. IEEE Transactions on Education 1988; 31(1): 32-34.

Biography:

Wu Jun Born in 1983, he received B.S. degree from Nanjing University of Aeronautics and Astronautics in 2005, and now is a Ph. D. candidate there. His main research interest lies in cooperative control.
E-mail: wj_nuaa@163.com